

Original Article
Pharmacology, Drug
Therapy & Toxicology



Vimentin Targeted Nano-gene Carrier for Treatment of Renal Diseases

Ansuja Pulickal Mathew ^{1,2}, Saji Uthaman ^{3*}, Eun Hui Bae ⁴, Jae Young Lee ⁵, and In-Kyu Park ^{1,2}

¹Department of Biomedical Sciences, Chonnam National University Medical School, Gwangju, Korea

²BioMedical Sciences Graduate Program (BMSGP), Chonnam National University, Hwasun, Korea

³Department of Polymer Science and Engineering, Chungnam National University, Daejeon, Korea

⁴Department of Internal Medicine, Chonnam National University Medical School, Gwangju, Korea

⁵School of Materials Science and Engineering, Gwangju Institute of Science and Engineering, Gwangju, Korea



Received: Aug 30, 2021

Accepted: Oct 21, 2021

Address for Correspondence:

In-Kyu Park, PhD

Department of Biomedical Sciences, Chonnam National University Medical School, BioMedical Sciences Graduate Program (BMSGP), Chonnam National University, 322 Seoyang-ro, Hwasun 58128, Republic of Korea.
E-mail: pik96@jnu.ac.kr

*Current address: Department of Chemical and Biological Engineering, Iowa State University, Ames 50011, USA

© 2021 The Korean Academy of Medical Sciences.

This is an Open Access article distributed under the terms of the Creative Commons Attribution Non-Commercial License (<https://creativecommons.org/licenses/by-nc/4.0/>) which permits unrestricted non-commercial use, distribution, and reproduction in any medium, provided the original work is properly cited.

ORCID iDs

Ansuja Pulickal Mathew

<https://orcid.org/0000-0001-5025-1623>

Saji Uthaman

<https://orcid.org/0000-0001-6387-7510>

Eun Hui Bae

<https://orcid.org/0000-0003-1727-2822>

Jae Young Lee

<https://orcid.org/0000-0003-4493-2494>

In-Kyu Park

<https://orcid.org/0000-0002-8522-8236>

ABSTRACT

Background: Chronic kidney disease (CKD) is a global health problem, and there is no permanent treatment for reversing kidney failure; thus, early diagnosis and effective treatment are required. Gene therapy has outstanding potential; however, the lack of safe gene delivery vectors, a reasonable transfection rate, and kidney targeting ability limit its application. Nanoparticles can offer innovative ways to diagnose and treat kidney diseases as they facilitate targetability and therapeutic efficacy.

Methods: Herein, we developed a proximal renal tubule-targeting gene delivery system based on alternative copolymer (PS) of sorbitol and polyethyleneimine (PEI), modified with vimentin-specific chitobionic acid (CA), producing PS-conjugated CA (PSC) for targeting toward vimentin-expressing cells in the kidneys. In vitro studies were used to determine cell viability, transfection efficiency, serum influence, and specific uptake in the human proximal renal tubular epithelial cell line (HK-2). Finally, the targeting efficiency of the prepared PSC gene carriers was checked in a murine model of Alport syndrome.

Results: Our results suggested that the prepared polyplex showed low cytotoxicity, enhanced transfection efficiency, specific uptake toward HK-2 cells, and excellent targeting efficiency toward the kidneys.

Conclusion: Collectively, from these results it can be inferred that the PSC can be further evaluated as a potential gene carrier for the kidney-targeted delivery of therapeutic genes for treating diseases.

Keywords: Kidney; Polyethyleneimine; Chitobionic Acid; Targeted Delivery; HK-2 Cells

INTRODUCTION

Chronic kidney disease (CKD) is an emerging health crisis, and it is possible to slow the progression by early diagnosis and treatment.¹ However, the strict and multilevel filtering mechanisms inherent to the kidneys play a crucial role in the success rate of the therapeutic systems.² Gene therapy, originally envisioned as an approach to treat genetic diseases, has been utilized as a strategy to cure acquired diseases by providing exogenous DNA via systemic or local delivery for expressing therapeutic proteins. Although many developments have been

Funding

This work was financially supported by the Bio & Medical Technology Development Program (No. NRF-2017M3A9E2056372) through the National Research Foundation of Korea (NRF) funded by the Korean government, MSIP. This work was also supported by the National Research Foundation of Korea (NRF) grant funded by the Korea government (MSIT) (No. 2020R1A2C2005620, 2020R1A5A2031185, NRF-2020M3A9G3080281 and NRF-2019M3E5D1A02068082). This study was also in part supported by a grant (No. BCRI20052) of Chonnam National University Hospital Biomedical Research Institute.

Disclosure

The authors have no potential conflicts of interest to disclose.

Author Contributions

Conceptualization: Bae EH, Lee JY, Park IK. Formal analysis: Mathew AP, Uthaman S. Investigation: Mathew AP, Uthaman S. Methodology: Mathew AP, Uthaman S. Supervision: Park IK. Writing - original draft: Mathew AP. Writing - review & editing: Mathew AP, Uthaman S, Park IK.

made over the past few years in gene delivery approaches toward treating diseases, very little progress has been made in treating renal diseases.³

Hydrodynamic approach or local administration has been used for gene delivery to the kidneys. However, this was associated with side effects and disadvantages, such as liver damage, kidney dysfunction, and invasiveness, limiting its clinical application.^{4,5} Both viral and non-viral gene delivery systems have been reported for the gene therapy of kidney diseases.⁶ Non-viral gene delivery systems based on liposomes,^{7,8} polyethyleneimine (PEI),⁹ and gelatin-based^{10,11} nanoparticles¹² have been reported but have faced challenges relating to in vivo delivery and specific targeting to the kidneys. An efficient gene delivery system should offer local transfer and expression of the therapeutic gene at the target tissue or organ.³ Thus, targeted delivery of therapeutics toward kidneys would be ideal for treating renal diseases as the effects would be limited to the kidneys and reduce any systemic toxicity.¹³⁻¹⁵

Nanoparticle-based targeted delivery systems can offer enhanced targeting to the kidneys via passive targeting by modulating the nanoparticle properties, such as size, surface charge, aspect ratio etc.¹⁶⁻¹⁸ Incorporating active targeting moieties to these nanoparticulate carriers can result in a successful and feasible strategy for more effective design of kidney specific nanoparticle.¹⁹ Active targeting via kidney-targeting peptides or antibodies that bind to specific receptors or ligands on specific kidney cells was performed previously.²⁰ Polymers, such as chitosan, were also found to show precise kidney targeting based on the megalin receptor-mediated endocytosis.^{14,21-24} Vimentin, an intermediate filament protein, is often visualized as a marker for epithelial to mesenchymal transition (EMT) on renal tubular epithelial cells in chronic renal diseases and can be considered a marker for tubular injury or renal dysfunction.^{25,26} Vimentins are also expressed in normal and carcinoma kidney tissues and in developing and adult kidneys.^{27,28} It was recently reported that vimentins show a lectin-like binding property and specifically bind to N-acetylglucosamine (GlcNAc).^{29,30} Later, it was established that the vimentin-expressing cells could also interact with GlcNAc-containing polymers.^{28,31,32} Because vimentin expression is also considered as a key marker for injured kidney tissues, utilizing the lectin binding-mediated uptake of nanoparticles would benefit kidney-targeted gene delivery by developing a nanocarrier modified with GlcNAc as the ligand, facilitating vimentin-mediated nanoparticle delivery to the injured site in kidney.

Non-viral gene delivery vectors, such as cationic PEI-based systems, are still considered as the gold standard because of their easy preparation, stability, and more straightforward modifications than other polymers.³³ PEI enables effectual DNA binding and protection and endosmotic ability, leading to better transfection efficiency. However, the non-degradable nature of PEI may often lead to toxicity, inhibiting its clinical applications.¹⁷ Moreover, high molecular weight PEI exhibits unwanted severe toxicity in addition to high transfection efficiency, compared to low molecular weight PEI.³⁴ Chemical modifications of PEI using degradable crosslinkers, such as diacrylate, introduce cleavable ester bonds to PEI, thus offering biodegradable properties. Moreover, the biodegradable cationic polymer interferes with normal cell functions less than other tightly binding polymers, resulting in reduced toxicity.³⁵ This degradable property of the polymer also enhances the efficient unpacking of DNA followed by efficient transcription of the released gene.^{35,36}

Sorbitol or D-glucitol, an organic osmolyte produced by plants, is non-toxic and thoroughly water-soluble. Sorbitol-based gene delivery systems have been documented in many previous studies.^{37,38} However, the osmotic activity of polysorbitols with many hydroxyl groups can

provide accelerated cellular uptake compared to sorbitol alone. The introduction of polysorbitols on PEI has been shown to result in enhanced transfection efficiency via accelerated cell uptake.³⁹⁻⁴³ In this regard, the combination of the osmotic activity of polysorbitol and the proton sponge effect of PEI can have a great potential as an excellent gene delivery system.

In the present study, we designed a chitobionic acid (CA)-based nanocarrier system for targeted gene delivery toward the kidneys. We utilized a low molecular weight PEI (LMWPEI), as they are less toxic compared to their high molecular weight counterparts. Initially, we prepared CA, a dimer of GlcNAc, via oxidation of chitobiose, and sorbitol diacrylate (SDA)-crosslinked PEI (PS) simultaneously. The PS was then conjugated with CA moieties via amide bond formation, resulting in PS-conjugated CA (PSC), the final kidney-targeted osmotically driven gene carrier. The vimentin targeting ability of the prepared PSC polymer was then exploited for developing a precise gene delivery system, which could specifically target the vimentin-expressing cells of kidneys, such as tubules and podocytes, during kidney disease.^{44,45} In the in vivo system, the CA moieties assist in enhanced targeting toward the kidneys via the lectin-like binding property of vimentin that enables it to bind to the GlcNAc moiety of CA as shown in Fig. 1. Here, the PS enables enhanced cellular uptake and transfection efficiency. The PS possesses ester linkages that are easily degradable via hydrolysis, resulting in low molecular weight non-toxic byproducts, thus, reducing cytotoxicity. In addition to the degradability, the hydroxyl groups of polysorbitol and the choice of LMWPEI, altogether support the reduced toxicity of PSC. Herein, we synthesized the PS polymer and modified it with CA resulting in PSC nanocarrier and investigated the physicochemical characterization and its efficiency as a gene carrier in human proximal renal tubular epithelial cells (HK-2). Later, we investigated the targeting ability of the nanocomplexes in Alport syndrome (AS) mice, a murine model of progressive CKD characterized by fibrosis.^{23,46} It is speculated that this gene delivery system can pave the way for rational therapeutic approaches for treating kidney diseases.

METHODS

Reagents and cell lines

Branched PEI (MW, 600 Da) was purchased from Polysciences, Inc. (Ambler, PA, USA), and SDA (MW, 290.27 Da) was purchased from Monomer-Polymer & Dajac Labs (Trevose, PA, USA). N-hydroxysuccinimide (98%) (NHS) and N-3-dimethyl aminopropyl-N-ethyl carbodiimide hydrochloride were purchased from Merck KGaA. 3-(4,5-Dimethylthiazol-2-yl)-5-(3-carboxymethoxyphenyl)-2-(4-sulfophenyl)-2H-tetrazolium) (MTS) was purchased from Promega (Madison, WI, USA). Chitobiose was purchased from Yaizu Suisankagaku Industry Co., Ltd. (Shizuoka, Japan). The luciferase plasmids (pDNA) transformed into competent DH5 α *Escherichia coli* cells via heat shock were grown in Luria–Bertani media containing kanamycin (100 μ g/mL; Biosesang Inc., Seongnam, Korea). The plasmids were extracted and purified with a plasmid purification kit (Intron Biotechnology, Co., Seongnam, Korea). The concentration of the purified plasmid was determined by absorbance at 260 nm using the NanoQuant app (Tecan, Männedorf, Switzerland). BOBO3 and DAPI were obtained from Thermo Fisher Scientific Korea Ltd. (Seoul, Korea). Other reagents used were of analytical grade and procured from commercial suppliers unless specified.

For cell culture, HK-2 cells were cultured in Dulbecco's modified Eagle's medium/nutrient mixture F-12 (DMEM F/12) purchased from WELGENE, South Korea and supplemented with

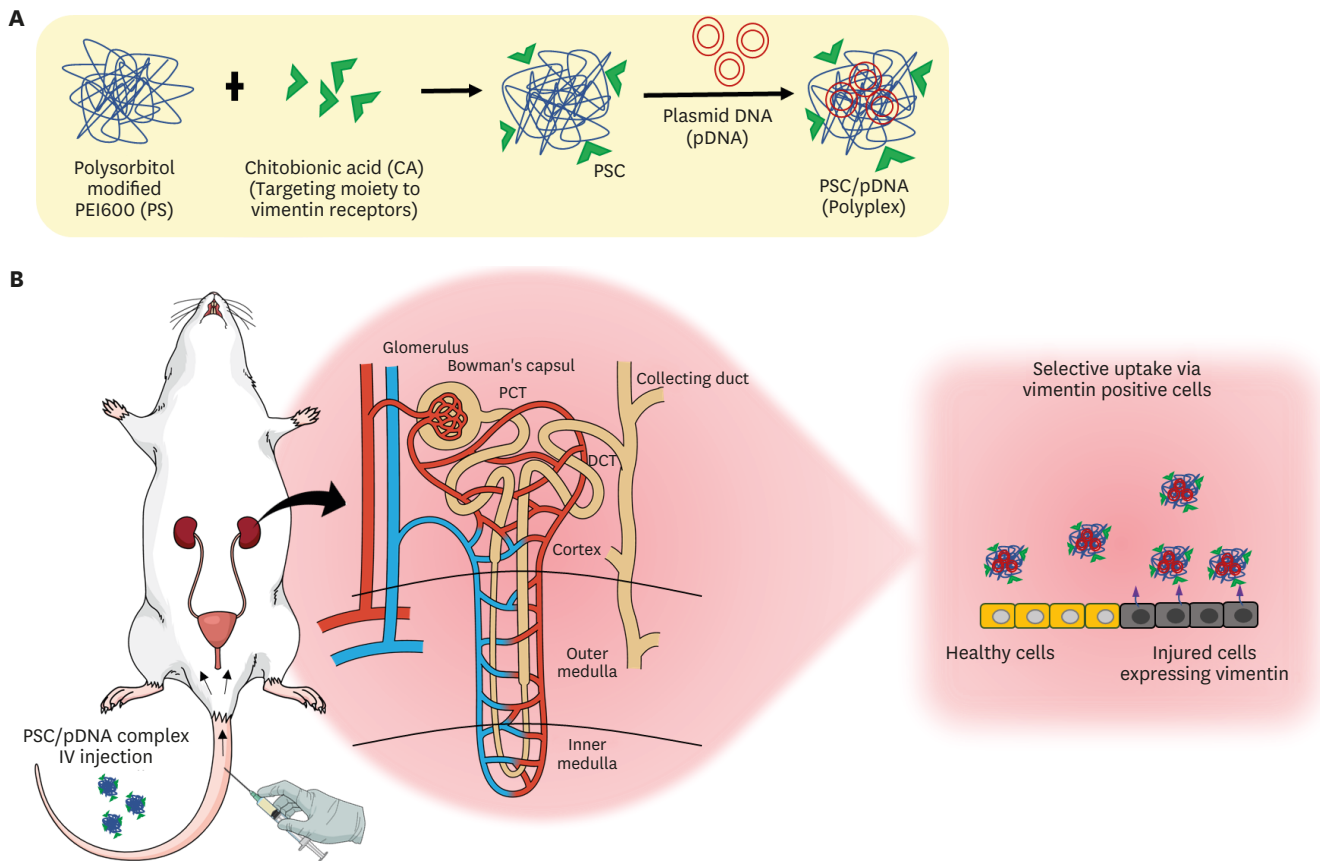


Fig. 1. Schematic representation showing (A) the preparation of PSC/pDNA nanocomplexes and (B) the mode of expression of PSC/pDNA nanocomplexes in the in vivo system.

PS = SDA crosslinked polyethyleneimine, PSC = PS-conjugated chitobionic acid, CA = chitobionic acid, PCT = proximal convoluted tubule, DCT = distal convoluted tubule.

10% fetal bovine serum and 1% antibiotics. The human breast adenocarcinoma (MCF-7) cells and human lung adenocarcinoma epithelial cells (A549) were cultured in Roswell Park Memorial Institute medium (WELGENE, Gyeongsan, Korea) and human embryonic kidney 293T cells (HEK293T) were cultured in Dulbecco's modified Eagle's medium supplemented with 10% fetal bovine serum and 1% antibiotics accordingly.

Cells were maintained at 37°C in a humidified atmosphere containing 5% CO₂, and the cell medium was changed every other day. Col4a3^{-/-} mice with a congenic 129X1/SvJ background were purchased from the Jackson Laboratory (Bar Harbor, ME, USA) and maintained under conventional conditions with free access to food and water.

Synthesis and characterization of CA, PS, and PSC

CA was prepared as previously described with slight modification.^{32,47,48} Briefly, chitobiose solution was prepared in 95% methanol and added dropwise into iodine solution prepared in 95% methanol at 40°C with proper stirring for 1 hour. The solution was removed from the heat, and potassium hydroxide solution prepared in methanol was added dropwise to the solution with stirring for 40 minutes until the brown solution became colorless. After cooling down, the sample was recrystallized using diethyl ether. The precipitated potassium chitobionate was then resuspended in a mixture of methanol and distilled water (1:5) and then passed through the Amberlite IR-120 (H⁺) column to obtain purified CA. The eluted sample was then lyophilized

and kept at -80°C until further use. The samples were characterized by Fourier-transform infrared (FT-IR) spectroscopy (PerkinElmer, Waltham, MA, USA).

PS was synthesized via the Michael addition reaction between PEI600 and SDA as previously reported.⁴⁹ Briefly, PEI and SDA at the mole ratio of 1:1 were dissolved separately in anhydrous DMSO. The SDA solution was added dropwise to PEI solution at 80°C with magnetic stirring under a nitrogen atmosphere. The reaction mixture was dialyzed against distilled water (MWCO, 1 kDa) at 4°C for 48 hours, lyophilized, and stored until further use. The PSC polymer was prepared by DCC/NHS reaction with a mole ratio of 1:2:2:5 for CA:DCC:NHS:PS in methanol as previously described.⁴⁷ The prepared CA, PS, and PSC chemical structures were confirmed using proton nuclear magnetic resonance ($^1\text{H NMR}$) spectroscopy (Bruker, Billerica, MA, USA).

Characterization of PSC/pDNA nanocomplexes

The ability of PSC to condense pDNA was evaluated using a gel retardation assay according to the N/P ratio (ratio of the amine groups of the polymers to the phosphate groups of pDNA). Briefly, the polymers at different predetermined concentrations were added to $1\ \mu\text{g}$ of pDNA according to a N/P molar ratio of up to 20. The mixture was then incubated for 30 minutes at room temperature (RT) and then made up to a total volume of $15\ \mu\text{L}$, inclusive of the gel loading dye. The nanocomplexes were then loaded onto a 1% agarose gel and run with Tris/acetate/EDTA buffer at 100 V for 30 minutes. The pDNA retardation was then observed by incubating the gel in red safe nucleic acid staining solution and visualizing by an electrophoresis gel documentation system.

Morphology, size, and surface charge of PSC/pDNA nanocomplexes

The hydrodynamic size and surface charge of the prepared PSC/pDNA nanocomplexes were checked using dynamic light scattering analysis (Zetasizer, Malvern, UK). The PSC/pDNA nanocomplex morphology was further observed using field emission transmission electron microscopy (FE-TEM, JEM-2100F; Jeol USA Inc., Peabody, MA, USA) with phosphotungstic acid negative staining.

In vitro cell viability studies

The in vitro cell viability was evaluated using the MTS cell proliferation assay kit in HK-2 cells. Briefly, 1×10^4 cells/well were seeded into 96-well plates in DMEM F12 medium and incubated overnight. The medium was aspirated and replaced with different concentrations of polymer-containing media. The samples were incubated for 4 hours and then replaced with fresh media and incubated for 24 hours. Then, $20\ \mu\text{L}$ of MTS reagent was added to each well and further incubated for 4 hours, and the absorbance was taken using a microplate spectrofluorometric reader (Tecan Spark®). In addition, we also checked the cell viability in other cell lines such as A549 and MCF-7 which does not express vimentin and HEK 293T cell line that express surface vimentins.^{50,51}

To check the cell viability with polymer/pDNA nanocomplexes, the polymer/pDNA nanocomplex was prepared as per the N/P ratio and incubated at RT for 30 minutes. The nanocomplexes were then made up with cell culture media, added to a 96-well plate and incubated for 4 hours. The media were aspirated and replaced with fresh media and further incubated for 24 hours followed by an MTS assay. Cell only and 0.1% Triton X-100 (Tx) were used as positive and negative controls for the study.

In vitro transfection efficiency study

To evaluate the transfection efficiency, HK-2 cells (5×10^4 cells/well) were seeded into 24-well cell culture plates and incubated overnight. The media were aspirated followed by the addition of polymer/pDNA nanocomplexes in media at various N/P ratios and incubated for 4 hours. The samples were then aspirated, new medium was added, and the samples were further incubated for 24 hours followed by luciferase assay. Briefly, cells were washed with DPBS followed by the addition of cell lysis buffer. The cells were kept at -80°C overnight and were later collected the supernatant, followed by luciferase substrate addition. The luminescence was observed using a multi-plate reader (Tecan, Spark 10M). Luminescence was normalized with total protein in the sample, and the transfection activity was expressed as relative light units per milligram of protein (RLU/mg). The transfection efficiency of the PSC/pDNA nanocomplexes was also determined in serum-free media and in the presence of CA. The transfection efficiency of PSC/pDNA nanocomplexes were also compared in A549 and HEK293T.

Cellular uptake studies

HK-2 (5×10^4 cells/well) cells were seeded into 8-well chamber slides and incubated overnight. The medium was aspirated, and the cells were treated with nanocomplexes formed with BOBO 3 dye-modified pDNA for 4 hours. Briefly, 30 μg of pDNA was mixed with 1 μL of BOBO 3 dye and stirred in the dark for 1 hour. The BOBO 3-modified pDNA was then utilized to prepare the nanocomplexes. The prepared nanocomplexes were added to cells and incubated for 4 hours. The media was removed, and the cells were washed with DPBS and fixed with 4% paraformaldehyde. The cells were rewashed with DPBS, counterstained with DAPI, and imaged using confocal laser scanning microscopy.

In vivo biodistribution studies

For biodistribution, the polymer PSC was modified with F-675 NIR dye. The synthesized PSC-F675 was then used for preparing the nanocomplexes. After 30 minutes at RT, the prepared nanocomplexes were administered intravenously via the tail vein of Alport mice. The mice were euthanized at 24 hours, and their organs were isolated. Fluorescence signals from the organs were analyzed using a fluorescence-labeled organism bio-imaging instrument (FOBI, NEO Science, Seoul, Korea).

Renal histology

To check the localization of the nanocomplexes in the kidneys, frozen sections (10 μm) of the excised kidneys were obtained. The frozen sections were counterstained with DAPI and visualized under a confocal laser scanning microscope.

Statistical analysis

The results were analyzed by GraphPad statistical software, and one-way analysis of variance was utilized for multiple comparisons among different groups. The results are expressed as the mean \pm standard deviation. Differences with *P* values of less than 0.05 were considered significant.

Ethics statement

All experimental protocols were undertaken according to the Institutional Animal Care and Use Committee of Chonnam National University Medical School (CNU IACUC-H-2020-25).

RESULTS

Synthesis and characterization of CA, PS, and PSC

CA was synthesized by the iodine/KOH-catalyzed oxidation of chitobiose^{45,48} and the chemical structure of the prepared CA was confirmed by comparing it with chitobiose via FTIR spectroscopy, which showed a peak at $1,737\text{ cm}^{-1}$, establishing the presence of carboxylate (Supplementary Fig. 1). PS was synthesized via the Michael addition reaction between the diacrylic group of SDA and amine groups of PEI600, resulting in degradable ester linkages. To prevent the hydrolysis of PS, the reaction was conducted in anhydrous DMSO, and to enhance the crosslinking efficiency, the reaction was performed at a high temperature. The formation of PS was then confirmed via NMR characterization.

As shown in Fig. 2A, the methylene protons of PEI at $\delta\ 2.2\text{--}2.5\text{ ppm}$ and vinyl groups of SDA around $5.8\text{--}6.8\text{ ppm}$ were observed. However, after conjugation, the peaks of vinyl protons disappeared, confirming the formation of PS. By integrating the methylene protons of PEI600 and SDA, the degree of substitution and mole percentage of SDA was calculated and found to be 78.5% and 43.97% respectively. PSC was synthesized by the DCC/NHS reaction forming amide linkages between the carboxylic group of CA and amine groups of PS. To confirm the formation of PS and PSC, the individual and final compounds were characterized by ^1H NMR spectroscopy. The conjugation of CA to PS was established by the presence of characteristic protons of the acetyl group ($\delta\ 1.9\text{--}2\text{ ppm}$) (Fig. 2B) of CA in PSC.^{45,47}

Physicochemical characterization of PSC/pDNA nanocomplexes

To confirm that PSC can efficiently condense pDNA, the ability of PSC to complex pDNA by electrostatic interaction was checked via gel retardation assay at various N/P ratios. Complexation was analyzed by the reduction in mobility of pDNA in agarose gel. It was observed that the migration of pDNA was completely retarded from the N/P ratio of 0.9, proving that PSC is remarkably effective in condensing pDNA and is an efficient gene carrier (Fig. 3A). To compare the superior ability of PSC in pDNA condensation we also compared the gel retardation with PEI600 and PEI25. From the data it was observed that the PEI600 showed complexation from N/P 5 whereas PEI25 showed complexation from N/P 0.9 like PSC. Thus, it can be concluded that PSC shows a strong pDNA condensation property like PEI25 but with less toxicity (Supplementary Fig. 2).

An effective gene delivery system requires efficient delivery and high uptake at the target cells, and physicochemical characteristics, such as particle size, surface charge, and shape,

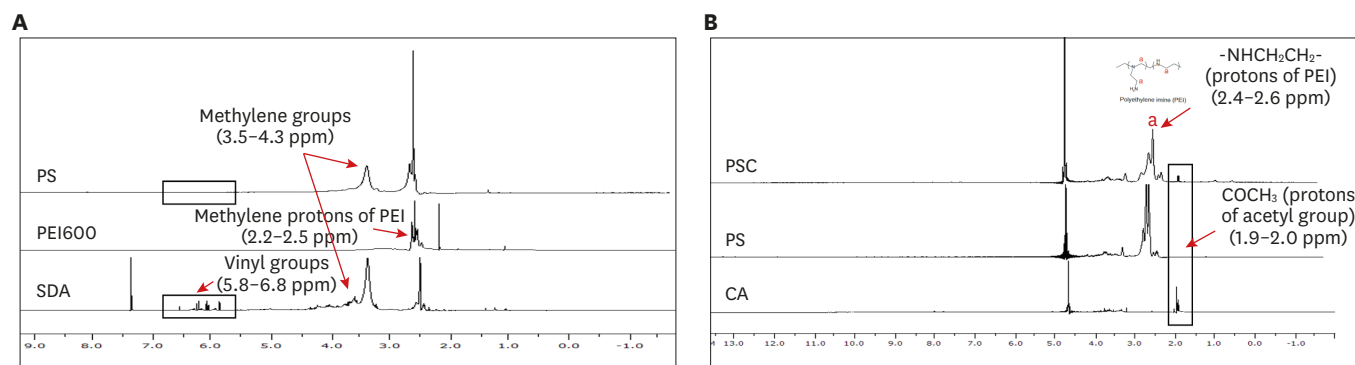


Fig. 2. Representative ^1H NMR spectra of SDA, PEI600, PS, CA, and PSC, confirming the formation of PS and PSC.

SDA = sorbitol diacrylate, PEI600 = polyethyleneimine 600 Da, PS = SDA crosslinked polyethyleneimine, CA = chitobionic acid, PSC = PS-conjugated chitobionic acid.

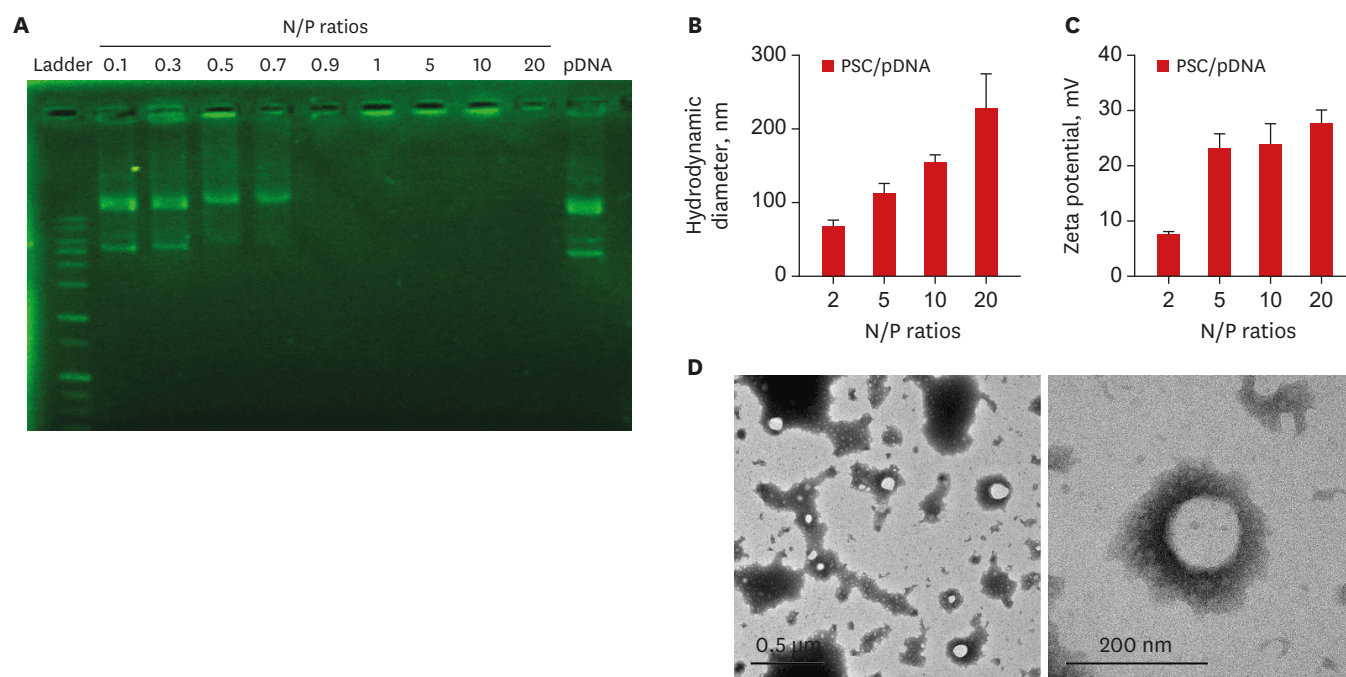


Fig. 3. Physicochemical characterizations of PSC/pDNA nanocomplexes (A) Agarose gel electrophoresis of PSC/pDNA nanocomplexes at various N/P ratios ranging from 0.1 to 20 with 1 μ g of pDNA. (B) The hydrodynamic diameter and (C) zeta potential measured at various N/P ratios from 2 to 20. (D) Field emission Transmission electron microscopy image of the PSC/pDNA complex of N/P 10 (low and high magnification images). PSC = PS-conjugated chitobionic acid.

of the nanocarrier are essential to achieve these properties.^{20,52} Thus, we analyzed the physicochemical characteristics such as size and surface charge of the prepared PSC/pDNA nanocomplexes. It was observed that the hydrodynamic diameter of the nanocomplexes ranged from 69 ± 7.1 to 228 ± 45.0 nm for the N/P ratio 1 to 20, as shown in Fig. 3B. The surface charge ranged from 7.7 ± 0.3 to 27.8 ± 2.3 mV (Fig. 3C). This could support the results of a previous study where it was confirmed that the size and surface charge of the polyplexes were increasing functions of the concentrations of PEI.⁵² The particle size was further confirmed by FE-TEM analysis. As shown in Fig. 3D, the PSC/pDNA showed a spherical morphology with an approximate size of 102.0 ± 12 nm. To address the stability of the PSC/pDNA complexes in the circulation, we further studied the size variation in the presence and absence of serum (Supplementary Fig. 3). No significant difference was observed in the hydrodynamic size up to 24 hours, however the size increased after 24 hours indicating the possibility of destabilization of PSC/pDNA complexes.

In vitro cell viability

An efficient delivery system should have low cytotoxicity so that it will elicit negligible side effects. Thus, the cell viability of the conjugated polymer was studied in vimentin-expressing HK-2 cells. The cell viability profile was compared with free polymers, such as PEI25 and PEI600, and conjugated counterparts, such as PS and PSC only (Fig. 4A). It was observed that the LMW PEI 600 was the least toxic, and PEI25 was the most toxic toward HK-2 cells. PS and PSC did not show much toxicity compared to PEI25, probably because of the presence of hydroxyl groups in the polymer. In addition, the cell viability of the final PSC polymer conjugate was also analyzed in HEK293T cell lines which are vimentin positive and vimentin negative cell lines such as MCF-7 and A549 to analyze the carrier toxicity (Supplementary Fig. 4). It was observed that the vimentin expressing HK2 and HEK293T showed a higher toxicity probably because of the enhanced uptake via vimentin.

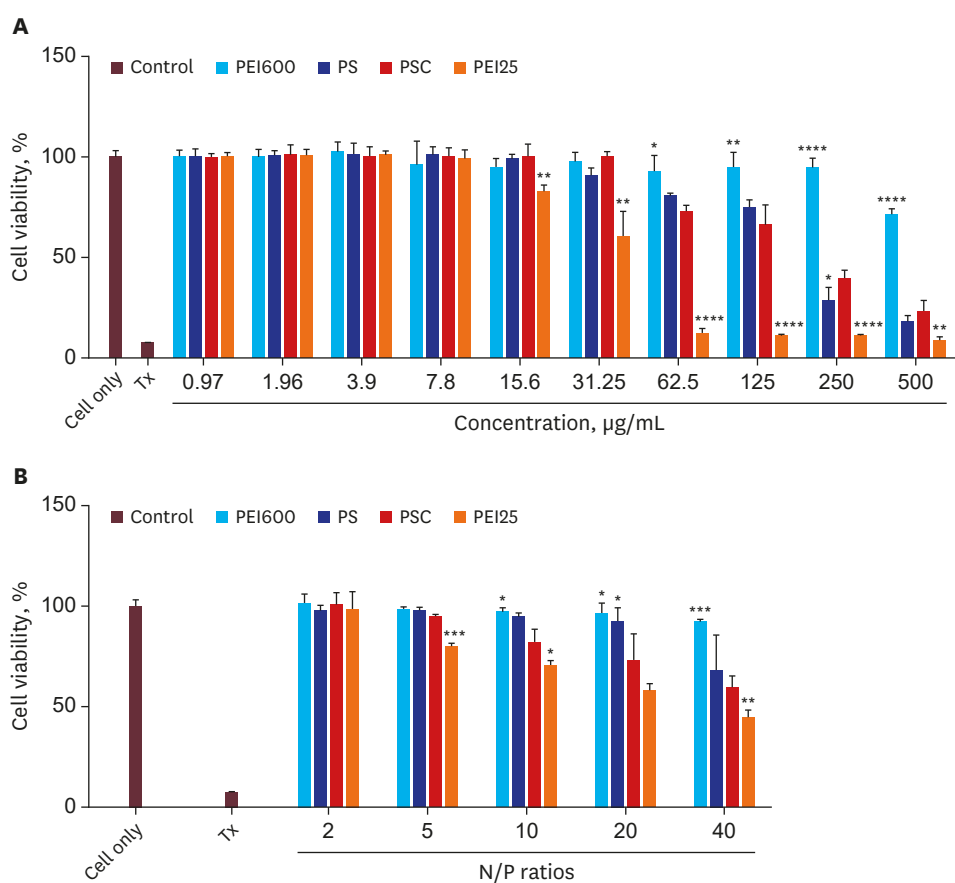


Fig. 4. Cell viability assay of (A) the polymer alone and (B) nanocomplexes at various N/P ratios in HK-2 cell lines (n = 3, error bars represent standard deviations).

PEI = polyethyleneimine, PS = SDA crosslinked polyethyleneimine, PSC = PS-conjugated chitobionic acid.

* $P < 0.05$, ** $P < 0.01$, *** $P < 0.001$, **** $P < 0.0001$.

Regardless of the group, all showed concentration-dependent toxicity to the cells. We also checked whether PSC showed any toxicity after pDNA complexation (Fig. 4B). The HK-2 cells were incubated with different polyplexes of N/P ratios up to 40. Like the polymer alone viability profile, the polymer pDNA complex also showed increased toxicity with increased N/P ratios. Polyplexes of PEI25 showed the lowest and PEI600 showed the highest cell viability.

In vitro transfection assay

We further evaluated the transfection efficiency of the nanocomplexes in HK-2 cells (Fig. 5A). The transfection efficiency of the prepared polyplexes can be affected under physiological conditions, such as the presence of serum in the in vivo conditions. The polyplexes may interact with the serum proteins, leading to instability that may affect the transfection efficiency. Hence, to confirm the effect of serum on the transfection efficiency, in vitro transfection was checked in the presence of serum. To mimic the physiological conditions, 10% FBS-containing media was utilized. Polyplex formed with PEI25 N/P 10 was used as the positive controls, and only pDNA and cells only were used as the negative controls for the study (Fig. 5B). It was observed that the transfection efficiency increased with an increased N/P ratio, and the highest N/P ratio was 20, which showed a higher transfection efficiency than the PEI25 positive control. In the case of transfection under serum conditions, the PSC/pDNA only showed a slight decrease,

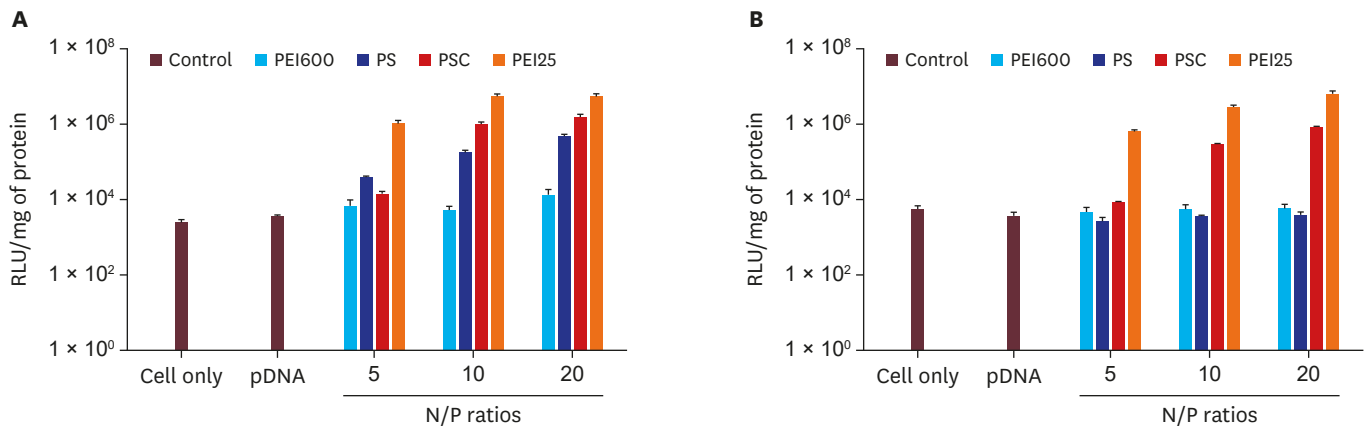


Fig. 5. Transfection efficiency of nanocomplexes at various N/P ratios in HK-2 cells **(A)** in the absence of serum **(B)** and in the presence of 10% FBS. PEI = polyethyleneimine, PS = SDA crosslinked polyethyleneimine, PSC = PS-conjugated chitobionic acid.

proving that the transfection efficiency was not particularly affected by the presence of serum. Hence, PSC/pDNA can be used as a gene carrier in vivo.

We further compared the transfection efficiency of PSC/pDNA in HK-2 cells (**Fig. 6A**) with that in MCF-7 cells (**Fig. 6B**), which is a breast cancer cell line deficient in vimentin expression.⁵³ Since the CA moieties on the PSC can help enhance targeting via the vimentin-CA interactions on the cell surface, the PSC/pDNA could show more specificity and improve transfection efficiency in HK-2 compared to MCF-7 cells. As shown in **Fig. 6**, a significant difference was observed with PSC/pDNA in the enhanced transfection compared to PS/pDNA, probably because of CA's targeting toward HK-2 cells. However, the transfection was considerably reduced in PSC/pDNA in MCF-7 due to the lack of vimentin expression. Thus, it can be speculated that the vimentin-mediated cellular uptake plays a role in the enhanced uptake of PSC/pDNA and thus it can be used as a suitable carrier for kidney targeting. Moreover, we compared the transfection efficiency of the final PSC/pDNA nanocomplexes in A549 and HEK293T cell lines. It was observed that the transfection efficiency of PSC/pDNA in A549 cell lines was very less (1.5×10^5) even at high N/P ratio compared to the very high transfection in HEK293T (8.6×10^8) which is believed to be a vimentin expressing kidney cell line (**Supplementary Fig. 5**).

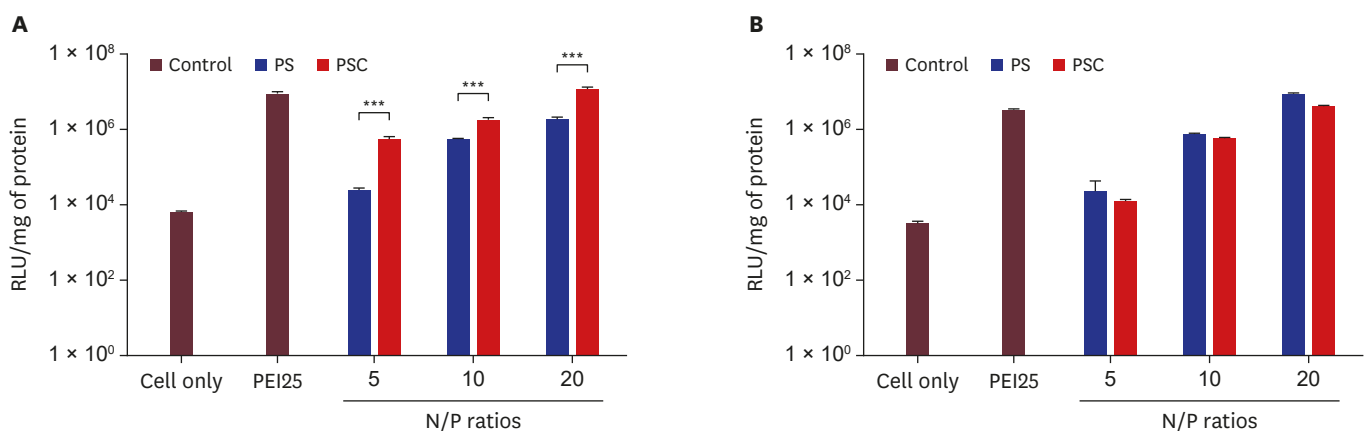


Fig. 6. Transfection efficiency of polyplexes at various N/P ratios in **(A)** HK-2 cells and **(B)** MCF-7 cells ($n = 3$, error bars represent standard deviations, $***P < 0.001$). PS = SDA crosslinked polyethyleneimine, PSC = PS-conjugated chitobionic acid, PEI = polyethyleneimine.

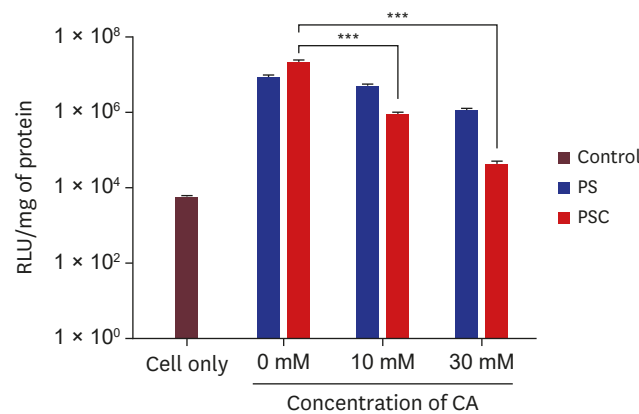


Fig. 7. Competition assay in the presence or absence of CA in HK-2 cells (n = 3, error bars represent standard deviations, ***P < 0.001).

PS = SDA crosslinked polyethyleneimine, PSC = PS-conjugated chitobionic acid, CA = chitobionic acid.

Competition assay

To further confirm the receptor-mediated uptake of the PSC/pDNA complexes, we performed a competition assay by pretreating the cells with CA before the transfection study. It was observed that the cells without prior CA treatment showed enhanced transfection after PSC/pDNA treatment; however, transfection gradually reduced after CA pretreatment because of the saturation of vimentin receptors by CA and reduced any further vimentin-mediated uptake (Fig. 7). PS/pDNA did not show much reduction in transfection efficiency, probably because of the lack of CA–vimentin interactions upon uptake.

Cellular uptake

To further confirm the cellular uptake of the PSC/pDNA polyplexes, HK-2 cells were incubated with polyplexes of different N/P ratios and the uptake efficiency was analyzed via confocal laser scanning microscopy. The BOBO 3-labeled pDNA was utilized for the preparation of the polyplexes. As observed in Fig. 8, the cellular uptake increased with increasing N/P ratios. The non-treated cells were used as the negative control. The N/P 5 showed significantly less fluorescence in the cells. However, when the N/P ratio reached 10, fluorescence increased, and no drastic difference in uptake was visible at N/P 20. We also confirmed the uptake by quantifying the fluorescence using ImageJ software. For all further studies, PSC/pDNA at N/P 10 was used.

In vivo biodistribution

To further check the targeting ability of the PSC/pDNA polyplexes, we modified PSC with the fluorescent dye Flamma 675 and performed biodistribution in Alport mice. After the intravenous injection of PSC-F675/pDNA polyplexes via the tail vein, the mice were euthanized at 24 hours, the organs were excised, and fluorescence imaging was performed using FOBI (NEO Science). As shown in Fig. 9, the highest fluorescence signal was observed from the kidneys, confirming that the polyplexes reached the kidneys more than any other organs, demonstrating the kidney targeting ability of PSC/pDNA polyplexes.

Renal histology

To determine the tissue localization of the PSC/pDNA polyplex, frozen sections of the isolated kidneys were prepared, and the fluorescence was observed under a confocal microscope (Fig. 10). The bright fluorescence in the inner cortical and outer medullary region of the PSC-F675/pDNA-injected mice confirmed the presence of the nanocarrier in these regions.

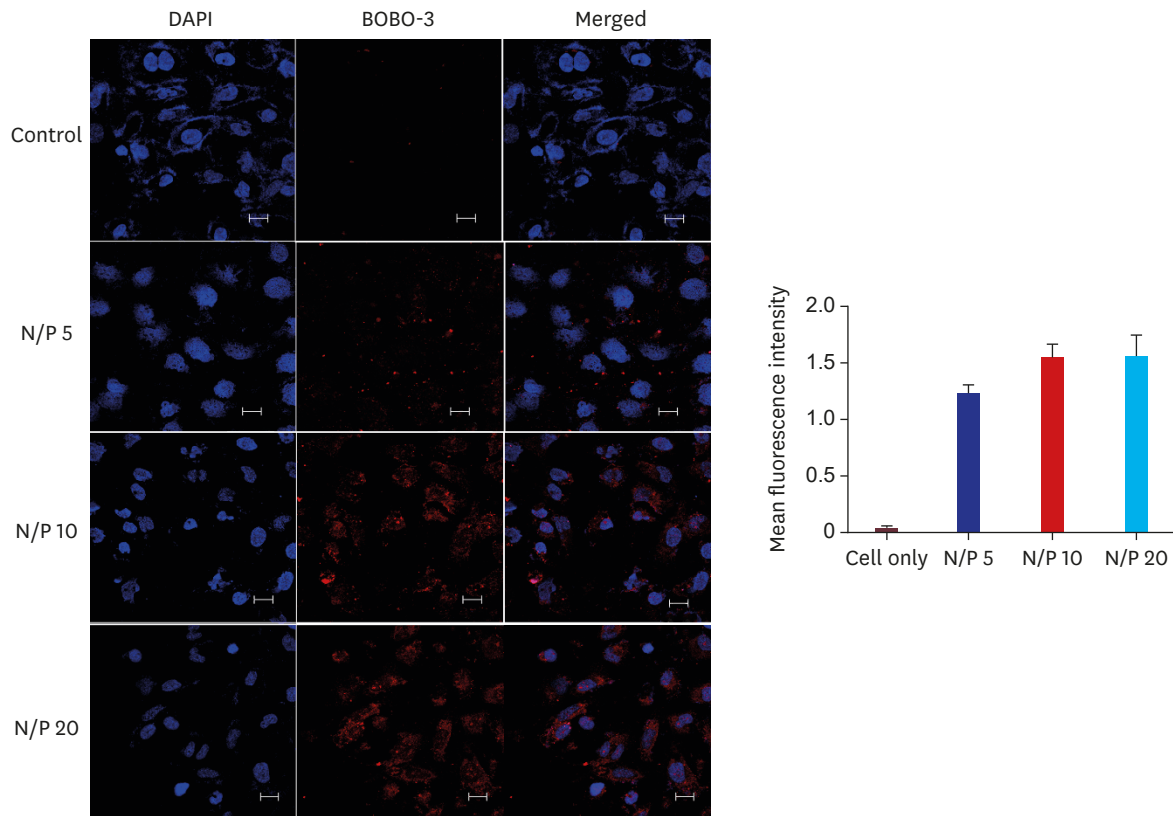


Fig. 8. Cellular uptake assessed in HK-2 cells after treatment with different N/P ratios for 4 hours (scale bar = 20 μ m).

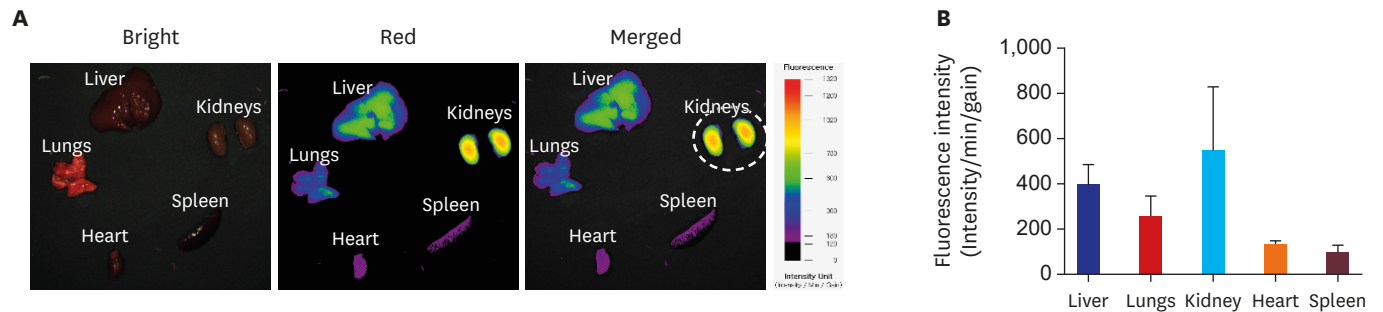


Fig. 9. (A) Ex vivo fluorescence images of isolated organs 24 hours after the intravenous injection of PSC-F675/pDNA nanocomplexes. (B) Quantification of fluorescence intensity from the organs.

Since vimentin expression would be upregulated in injured tubule cells and glomeruli of AS,^{44,54} this result can suggest the possibility of vimentin mediated uptake of the polyplexes via tubules or glomeruli. Thus, it can be concluded that the PSC nanocarrier can be utilized as an efficient gene carrier for targeted delivery to the kidneys. This gene carrier can be further utilized for therapeutic studies by delivering therapeutic genes.

DISCUSSION

Our group has previously proved the excellent ability of polysorbitols to enhance the transfection efficiency of the PEI-mediated gene carrier.⁴⁰⁻⁴² Here, a LMWPEI-based gene

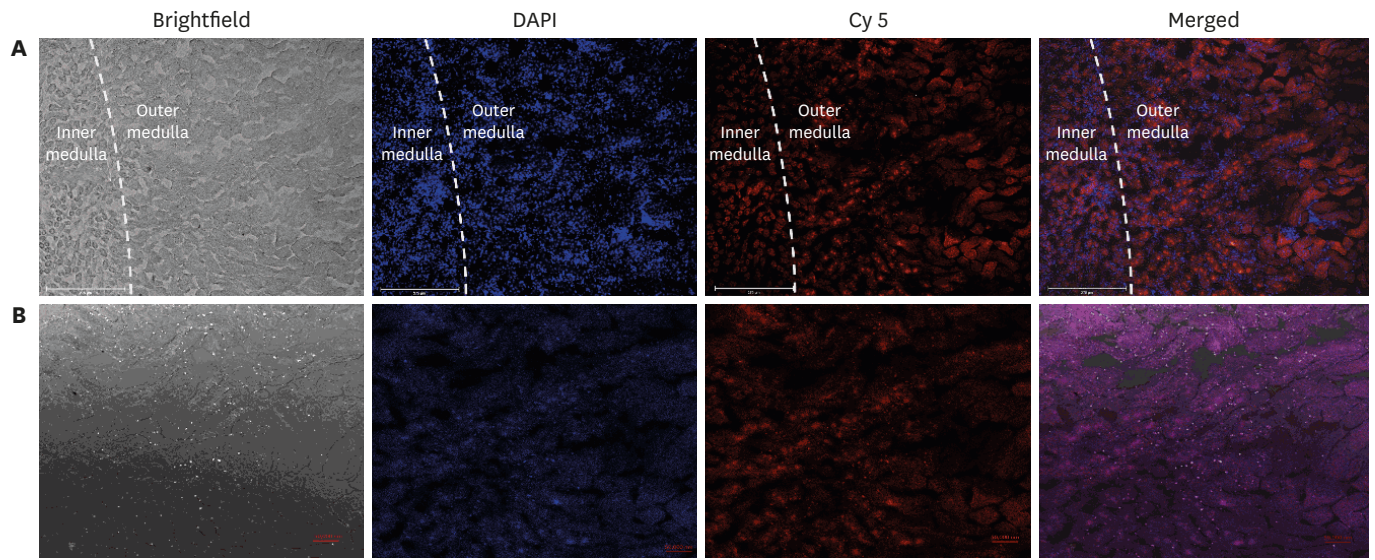


Fig. 10. Histology examination of kidney sections by confocal microscopy showing the presence of accumulated PSC-F675/pDNA in the kidneys **(A)** 20× magnification **(B)** 40× magnification.

carrier was developed based on PEI600 and SDA and was further modified by the targeting moiety CA. Vimentins are intermediate filaments with a significant role in maintaining cytoplasmic structures and play an important role in cell division and migration.²⁹ However, it can be exposed on the surface of specific cells under normal or some pathophysiological conditions. Under certain conditions, it has been proposed to act as a receptor or co-receptor for multiple viruses.⁵⁵ Thus, the role of vimentin during EMT is known; however, its role in kidney diseases and its relevance in formulating kidney-targeted gene carrier systems have not been explored widely. Here, we prepared PSC/pDNA nanocomplexes and performed *in vitro* cell studies in kidney proximal tubule cells, which are vimentin-positive cells, and completed *in vivo* biodistribution to confirm the accumulation of PSC/pDNA nanocomplexes in the kidneys. First, we established the conjugation of the CA moieties on the PSC polymer, and then we further evaluated the ability of the modified PSC polymer in the formation of polyplexes. We checked different N/P ratios to optimize the polymer ratios for formulating stable polyplexes. The physicochemical characterization of the formed polyplexes confirmed that PSC could efficiently condense the polymer above N/P 0.9. The particle size of the prepared polyplexes increased with the N/P ratio. However, N/P 10 showed a hydrodynamic size at around 150 nm.

Since the particle size below 200 nm is beneficial for cell uptake via endocytosis, we expect that these polyplexes will be taken up quickly by cells. FE-TEM images also confirmed the particle size to be less than 200 nm; hence, it is believed that these polyplexes can access the kidneys through proximal tubule cells.²⁰ *In vitro* cell studies further showed that the cytotoxicity of the PS, PSC, and polyplexes was less compared to that of the standard polymeric carrier PEI25. The toxicity of PEI25 and low transfection efficiency of LMWPEI are the two major concerns in the development of an effective PEI-based gene carrier. Since PS and PSC showed less toxicity compared to PEI25, it was noted that the prepared PS and PSC might have degraded due to the cleavable ester linkages and were not aggregated at the cell surface to impart toxicity. Moreover, the presence of hydroxyl groups on polysorbitols also involved in the reduced toxicity.⁴⁰

The luciferase assay of various polyplexes confirmed that the PSC polymer showed higher transfection efficiency compared to the unmodified PS in HK-2 cells; however, no significant

difference between PS and PSC was observed in the vimentin-negative MCF-7 cells. We also observed that the transfection efficiency of PSC/pDNA was not compromised by the presence of serum; however, the transfection efficiency was reduced after pretreatment with CA. On the other hand, PS/pDNA did not show a considerable difference in the transfection efficiency after CA pretreatment suggesting that PS has no affinity toward surface vimentins on cells. This study thus confirms the role of CA–vimentin interactions in cell uptake and the subsequent enhanced transfection efficiency. To visualize the cellular fate of PSC/pDNA complexes, we assessed the cellular uptake of PSC/pDNA complexes after modifying the pDNA with DNA intercalating dye. The red fluorescence of pDNA inside the cells confirmed the presence of polyplexes. It was also observed that the fluorescence was distributed in the cytoplasm and the nucleus after 4 hours of treatment, concluding that the polyplex must have released the pDNA to be transported into the nucleus for gene expression. Finally, we checked the kidney-targeting ability of PSC/pDNA polyplexes in an animal model of human AS. This murine model is characterized by progressive renal disease and tubulointerstitial kidney fibrosis and, vimentin expression is inevitable during kidney fibrosis.^{23,56} The high fluorescence intensity in the kidneys measured from the ex vivo organs suggested that the PSC/pDNA complexes successfully accumulated in the kidneys. The localization of the PSC/pDNA complexes inside the kidneys was further analyzed by the histological examination of frozen sections. The confocal images concluded that the PSC-F675/pDNA fluorescent gene carrier was localized around the inner medulla and outer cortical regions of the kidneys where the tubules, glomeruli and peritubular capillaries are distributed.

Although our results suggest targeted gene delivery toward the kidneys, this should be further investigated in other disease models as should its efficiency in therapeutic studies. In conclusion, we report a kidney-specific targeted system for gene delivery. This PSC/pDNA-mediated gene carrier system is expected to be a safe and effective strategy for developing a kidney-targeted gene delivery system.

SUPPLEMENTARY MATERIALS

Supplementary Fig. 1

Fourier-transform infrared analysis of chitobiose and chitobionic acid.

[Click here to view](#)

Supplementary Fig. 2

Agarose gel electrophoresis of (A) PEI600/pDNA and (B) PEI25/pDNA polyplexes at various N/P ratios ranging from 0.1 to 20 with 1 µg pDNA (L-Ladder).

[Click here to view](#)

Supplementary Fig. 3

Stability of PSC/pDNA nanocomplexes upto 48 hours in DW and 10% FBS.

[Click here to view](#)

Supplementary Fig. 4

Cell viability of PSC at different concentration in different cell lines.

[Click here to view](#)

Supplementary Fig. 5

Transfection efficiency of PSC in A549 and HEK293T cell lines.

[Click here to view](#)**REFERENCES**

1. Levey AS, Atkins R, Coresh J, Cohen EP, Collins AJ, Eckardt KU, et al. Chronic kidney disease as a global public health problem: approaches and initiatives - a position statement from Kidney Disease Improving Global Outcomes. *Kidney Int* 2007;72(3):247-59.
[PUBMED](#) | [CROSSREF](#)
2. Boron WF, Boulpaep EL. *Medical Physiology E-book*. Philadelphia, PA, USA: Elsevier Health Sciences; 2016.
3. Tomasoni S, Benigni A. Gene therapy: how to target the kidney. Promises and pitfalls. *Curr Gene Ther* 2004;4(1):115-22.
[PUBMED](#) | [CROSSREF](#)
4. Hamar P, Song E, Kökény G, Chen A, Ouyang N, Lieberman J. Small interfering RNA targeting Fas protects mice against renal ischemia-reperfusion injury. *Proc Natl Acad Sci U S A* 2004;101(41):14883-8.
[PUBMED](#) | [CROSSREF](#)
5. Takabatake Y, Isaka Y, Mizui M, Kawachi H, Takahara S, Imai E. Chemically modified siRNA prolonged RNA interference in renal disease. *Biochem Biophys Res Commun* 2007;363(2):432-7.
[PUBMED](#) | [CROSSREF](#)
6. Miyazawa H, Hirai K, Ookawara S, Ishibashi K, Morishita Y. Nano-sized carriers in gene therapy for renal fibrosis *in vivo*. *Nano Rev Exp* 2017;8(1):1331099.
[PUBMED](#) | [CROSSREF](#)
7. Lai LW, Moeckel GW, Lien YH. Kidney-targeted liposome-mediated gene transfer in mice. *Gene Ther* 1997;4(5):426-31.
[PUBMED](#) | [CROSSREF](#)
8. Ito K, Chen J, Asano T, Vaughan ED Jr, Poppas DP, Hayakawa M, et al. Liposome-mediated gene therapy in the kidney. *Hum Cell* 2004;17(1):17-28.
[PUBMED](#) | [CROSSREF](#)
9. Morishita Y, Imai T, Yoshizawa H, Watanabe M, Ishibashi K, Muto S, et al. Delivery of microRNA-146a with polyethylenimine nanoparticles inhibits renal fibrosis *in vivo*. *Int J Nanomedicine* 2015;10:3475-88.
[PUBMED](#) | [CROSSREF](#)
10. Xia Z, Abe K, Furusu A, Miyazaki M, Obata Y, Tabata Y, et al. Suppression of renal tubulointerstitial fibrosis by small interfering RNA targeting heat shock protein 47. *Am J Nephrol* 2008;28(1):34-46.
[PUBMED](#) | [CROSSREF](#)
11. Aoyama T, Yamamoto S, Kanematsu A, Ogawa O, Tabata Y. Local delivery of matrix metalloproteinase gene prevents the onset of renal sclerosis in streptozotocin-induced diabetic mice. *Tissue Eng* 2003;9(6):1289-99.
[PUBMED](#) | [CROSSREF](#)
12. Pillarisetti S, Uthaman S, Huh KM, Koh YS, Lee S, Park IK. Multimodal composite iron oxide nanoparticles for biomedical applications. *Tissue Eng Regen Med* 2019;16(5):451-65.
[PUBMED](#) | [CROSSREF](#)
13. Imai E, Takabatake Y, Mizui M, Isaka Y. Gene therapy in renal diseases. *Kidney Int* 2004;65(5):1551-5.
[PUBMED](#) | [CROSSREF](#)
14. Kim CS, Mathew AP, Uthaman S, Moon MJ, Bae EH, Kim SW, et al. Glycol chitosan-based renal docking biopolymeric nanomicelles for site-specific delivery of the immunosuppressant. *Carbohydr Polym* 2020;241:116255.
[PUBMED](#) | [CROSSREF](#)
15. Lee JN, Chun SY, Ha YS, Choi KH, Yoon GS, Kim HT, et al. Target molecule expression profiles in metastatic renal cell carcinoma: development of individual targeted therapy. *Tissue Eng Regen Med* 2016;13(4):416-27.
[PUBMED](#) | [CROSSREF](#)
16. Singh RK, Kim HW. Inorganic nanobiomaterial drug carriers for medicine. *Tissue Eng Regen Med* 2013;10(6):296-309.
[CROSSREF](#)

17. Longmire MR, Ogawa M, Choyke PL, Kobayashi H. Biologically optimized nanosized molecules and particles: more than just size. *Bioconjug Chem* 2011;22(6):993-1000.
[PUBMED](#) | [CROSSREF](#)
18. Mohanty A, Uthaman S, Park IK. Utilization of polymer-lipid hybrid nanoparticles for targeted anti-cancer therapy. *Molecules* 2020;25(19):4377.
[PUBMED](#) | [CROSSREF](#)
19. Choi H, Choi Y, Yim HY, Mirzaaghasi A, Yoo JK, Choi C. Biodistribution of exosomes and engineering strategies for targeted delivery of therapeutic exosomes. *Tissue Eng Regen Med* 2021;18(4):499-511.
[PUBMED](#) | [CROSSREF](#)
20. Huang Y, Wang J, Jiang K, Chung EJ. Improving kidney targeting: The influence of nanoparticle physicochemical properties on kidney interactions. *J Control Release* 2021;334:127-37.
[PUBMED](#) | [CROSSREF](#)
21. Yang C, Nilsson L, Cheema MU, Wang Y, Frøkiær J, Gao S, et al. Chitosan/siRNA nanoparticles targeting cyclooxygenase type 2 attenuate unilateral ureteral obstruction-induced kidney injury in mice. *Theranostics* 2015;5(2):110-23.
[PUBMED](#) | [CROSSREF](#)
22. Gao S, Hein S, Dagnæs-Hansen F, Weyer K, Yang C, Nielsen R, et al. Megalin-mediated specific uptake of chitosan/siRNA nanoparticles in mouse kidney proximal tubule epithelial cells enables AQP1 gene silencing. *Theranostics* 2014;4(10):1039-51.
[PUBMED](#) | [CROSSREF](#)
23. Suh SH, Mathew AP, Choi HS, Vasukutty A, Kim CS, Kim IJ, et al. Kidney-accumulating olmesartan-loaded nanomicelles ameliorate the organ damage in a murine model of Alport syndrome. *Int J Pharm* 2021;600:120497.
[PUBMED](#) | [CROSSREF](#)
24. Kim CS, Mathew AP, Vasukutty A, Uthaman S, Joo SY, Bae EH, et al. Glycol chitosan-based tacrolimus-loaded nanomicelle therapy ameliorates lupus nephritis. *J Nanobiotechnology* 2021;19(1):109.
[PUBMED](#) | [CROSSREF](#)
25. Vanstherthem D, Gossiaux A, Declèves AE, Caron N, Nonclercq D, Legrand A, et al. Expression of nestin, vimentin, and NCAM by renal interstitial cells after ischemic tubular injury. *J Biomed Biotechnol* 2010;2010:193259.
[PUBMED](#) | [CROSSREF](#)
26. Holthöfer H, Miettinen A, Lehto VP, Lehtonen E, Virtanen I. Expression of vimentin and cytokeratin types of intermediate filament proteins in developing and adult human kidneys. *Lab Invest* 1984;50(5):552-9.
[PUBMED](#)
27. Beham A, Ratschek M, Zatloukal K, Schmid C, Denk H. Distribution of cytokeratins, vimentin and desmoplakins in normal renal tissue, renal cell carcinomas and oncocytoma as revealed by immunofluorescence microscopy. *Virchows Arch A Pathol Anat Histopathol* 1992;421(3):209-15.
[PUBMED](#) | [CROSSREF](#)
28. Skinnider BF, Folpe AL, Hennigar RA, Lim SD, Cohen C, Tamboli P, et al. Distribution of cytokeratins and vimentin in adult renal neoplasms and normal renal tissue: potential utility of a cytokeratin antibody panel in the differential diagnosis of renal tumors. *Am J Surg Pathol* 2005;29(6):747-54.
[PUBMED](#) | [CROSSREF](#)
29. Ise H, Kobayashi S, Goto M, Sato T, Kawakubo M, Takahashi M, et al. Vimentin and desmin possess GlcNAc-binding lectin-like properties on cell surfaces. *Glycobiology* 2010;20(7):843-64.
[PUBMED](#) | [CROSSREF](#)
30. Aso S, Ise H, Takahashi M, Kobayashi S, Morimoto H, Izawa A, et al. Effective uptake of N-acetylglucosamine-conjugated liposomes by cardiomyocytes in vitro. *J Control Release* 2007;122(2):189-98.
[PUBMED](#) | [CROSSREF](#)
31. Singh B, Maharjan S, Kim YK, Jiang T, Islam MA, Kang SK, et al. Targeted gene delivery via N-acetylglucosamine receptor mediated endocytosis. *J Nanosci Nanotechnol* 2014;14(11):8356-64.
[PUBMED](#) | [CROSSREF](#)
32. Kim SJ, Ise H, Goto M, Komura K, Cho CS, Akaike T. Gene delivery system based on highly specific recognition of surface-vimentin with N-acetylglucosamine immobilized polyethylenimine. *Biomaterials* 2011;32(13):3471-80.
[PUBMED](#) | [CROSSREF](#)
33. Lungwitz U, Breunig M, Blunk T, Göpferich A. Polyethylenimine-based non-viral gene delivery systems. *Eur J Pharm Biopharm* 2005;60(2):247-66.
[PUBMED](#) | [CROSSREF](#)

34. Fischer D, Bieber T, Li Y, Elsässer HP, Kissel T. A novel non-viral vector for DNA delivery based on low molecular weight, branched polyethylenimine: effect of molecular weight on transfection efficiency and cytotoxicity. *Pharm Res* 1999;16(8):1273-9.
[PUBMED](#) | [CROSSREF](#)
35. Forrest ML, Koerber JT, Pack DW. A degradable polyethylenimine derivative with low toxicity for highly efficient gene delivery. *Bioconjug Chem* 2003;14(5):934-40.
[PUBMED](#) | [CROSSREF](#)
36. Ahn CH, Chae SY, Bae YH, Kim SW. Biodegradable poly(ethylenimine) for plasmid DNA delivery. *J Control Release* 2002;80(1-3):273-82.
[PUBMED](#) | [CROSSREF](#)
37. Maiti KK, Lee WS, Takeuchi T, Watkins C, Fretz M, Kim DC, et al. Guanidine-containing molecular transporters: sorbitol-based transporters show high intracellular selectivity toward mitochondria. *Angew Chem Int Ed Engl* 2007;46(31):5880-4.
[PUBMED](#) | [CROSSREF](#)
38. Shaikh SF, Mane RS, Min BK, Hwang YJ, Joo O. D-sorbitol-induced phase control of TiO₂ nanoparticles and its application for dye-sensitized solar cells. *Sci Rep* 2016;6(1):1-10.
[PUBMED](#) | [CROSSREF](#)
39. Islam MA, Yun CH, Choi YJ, Shin JY, Arote R, Jiang HL, et al. Accelerated gene transfer through a polysorbitol-based transporter mechanism. *Biomaterials* 2011;32(36):9908-24.
[PUBMED](#) | [CROSSREF](#)
40. Islam MA, Shin JY, Firdous J, Park TE, Choi YJ, Cho MH, et al. The role of osmotic polysorbitol-based transporter in RNAi silencing via caveolae-mediated endocytosis and COX-2 expression. *Biomaterials* 2012;33(34):8868-80.
[PUBMED](#) | [CROSSREF](#)
41. Islam MA, Shin JY, Yun CH, Cho CS, Seo HW, Chae C, et al. The effect of RNAi silencing of p62 using an osmotic polysorbitol transporter on autophagy and tumorigenesis in lungs of K-rasLA1 mice. *Biomaterials* 2014;35(5):1584-96.
[PUBMED](#) | [CROSSREF](#)
42. Cho WY, Hong SH, Singh B, Islam MA, Lee S, Lee AY, et al. Suppression of tumor growth in lung cancer xenograft model mice by poly(sorbitol-co-PEI)-mediated delivery of osteopontin siRNA. *Eur J Pharm Biopharm* 2015;94:450-62.
[PUBMED](#) | [CROSSREF](#)
43. Nguyen KC, Muthiah M, Islam MA, Kalash RS, Cho CS, Park H, et al. Selective transfection with osmotically active sorbitol modified PEI nanoparticles for enhanced anti-cancer gene therapy. *Colloids Surf B Biointerfaces* 2014;119:126-36.
[PUBMED](#) | [CROSSREF](#)
44. Steenhard BM, Vanacore R, Friedman D, Zelenchuk A, Stroganova L, Isom K, et al. Upregulated expression of integrin α 1 in mesangial cells and integrin α 3 and vimentin in podocytes of Col4a3-null (Alport) mice. *PLoS One* 2012;7(12):e50745.
[PUBMED](#) | [CROSSREF](#)
45. Kim YK, Singh B, Jiang HL, Park TE, Jiang T, Park IK, et al. N-Acetylglucosamine-conjugated block copolymer consisting of poly(ethylene oxide) and cationic polyaspartamide as a gene carrier for targeting vimentin-expressing cells. *Eur J Pharm Sci* 2014;51:165-72.
[PUBMED](#) | [CROSSREF](#)
46. Van Nguyen TT, Vu NB, Van Pham P. Mesenchymal stem cell transplantation for ischemic diseases: mechanisms and challenges. *Tissue Eng Regen Med* 2021;18(4):587-611.
[PUBMED](#) | [CROSSREF](#)
47. Islam MA, Kim S, Firdous J, Lee AY, Hong SH, Seo MK, et al. A high affinity kidney targeting by chitobionic acid-conjugated polysorbitol gene transporter alleviates unilateral ureteral obstruction in rats. *Biomaterials* 2016;102:43-57.
[PUBMED](#) | [CROSSREF](#)
48. Kaifu R, Goldstein IJ. N,N'-Diacylchitobionic N-alkylamides: synthesis, and interaction with two 2-acetamido-2-deoxy-D-glucose-binding lectins. *Carbohydr Res* 1981;96(2):241-7.
[PUBMED](#) | [CROSSREF](#)
49. Luu QP, Shin JY, Kim YK, Islam MA, Kang SK, Cho MH, et al. High gene transfer by the osmotic polysorbitol-mediated transporter through the selective caveolae endocytic pathway. *Mol Pharm* 2012;9(8):2206-18.
[PUBMED](#) | [CROSSREF](#)
50. Inada M, Izawa G, Kobayashi W, Ozawa M. 293 cells express both epithelial as well as mesenchymal cell adhesion molecules. *Int J Mol Med* 2016;37(6):1521-7.
[PUBMED](#) | [CROSSREF](#)

51. Ooi A, Wong A, Esau L, Lemtiri-Chlieh F, Gehring C. A guide to transient expression of membrane proteins in HEK-293 cells for functional characterization. *Front Physiol* 2016;7:300.
[PUBMED](#) | [CROSSREF](#)
52. Hou S, Ziebac N, Wiczorek SA, Kalwarczyk E, Sashuk V, Kalwarczyk T, et al. Formation and structure of PEI/DNA complexes: quantitative analysis. *Soft Matter* 2011;7(15):6967-72.
[CROSSREF](#)
53. Hendrix MJ, Seftor EA, Seftor RE, Trevor KT. Experimental co-expression of vimentin and keratin intermediate filaments in human breast cancer cells results in phenotypic interconversion and increased invasive behavior. *Am J Pathol* 1997;150(2):483-95.
[PUBMED](#)
54. Kusaba T, Lalli M, Kramann R, Kobayashi A, Humphreys BD. Differentiated kidney epithelial cells repair injured proximal tubule. *Proc Natl Acad Sci U S A* 2014;111(4):1527-32.
[PUBMED](#) | [CROSSREF](#)
55. Ramos I, Stamatakis K, Oeste CL, Pérez-Sala D. Vimentin as a multifaceted player and potential therapeutic target in viral infections. *Int J Mol Sci* 2020;21(13):4675.
[PUBMED](#) | [CROSSREF](#)
56. Wang Z, Divanyan A, Jourdeuil FL, Goldman RD, Ridge KM, Jourdeuil D, et al. Vimentin expression is required for the development of EMT-related renal fibrosis following unilateral ureteral obstruction in mice. *Am J Physiol Renal Physiol* 2018;315(4):F769-80.
[PUBMED](#) | [CROSSREF](#)